

Augmented atmospheric chemistry of nitrous oxide and its potentially important implications for global change modeling

Sheo S. Prasad

Creative Research Enterprises, Pleasanton, CA 94566, USA

e-mail: ssp@CreativeResearch.org; Ph: 925 426 9341

and

Edward C. Zipf

Innovative Science & Technology, Inc

Pittsburgh, PA 15238

e-mail: Edczipf@aol.com; Ph: 412 963 6493

Index: 0340, 0322, 0330, 0485, 1610

ABSTRACT

Nitrous oxide (N_2O) is a significant atmospheric constituent included in the Kyoto Protocol. Here, in the context of the science of global change, we show that there is a consequential atmospheric production of N_2O . Most of the production is in the troposphere as consequence of O_3 excitation by Huggins band. Stratospheric production from highly vibrationally excited nascent O_3 is comparatively smaller. Due to their photochemical origin, these productions have a significant seasonal and latitudinal dependence. Inverse modeling of N_2O , neglecting these N_2O productions, run the risk that the estimated globally averaged emission of N_2O (from microbial and anthropogenic activity) could be in error by about 7%. The seasonality and the latitudinal dependence of the emissions could be in greater error. Neglect of tropospheric production of N_2O from excited O_3 may be tolerable in modeling the present atmosphere, since N_2O is an observed constituent. However, that neglect can put forecasting of global change at risk since surface emission and the tropospheric production of N_2O differ in the causes and rates of growth. Comparisons of the modeled and observed volume mixing ratios of N_2O show overestimation and underestimation by models depending on the latitude and season. Global averaging, to reduce the effects of uncertainties in model dynamics, reveals N_2O -source deficit in the stratosphere and implies production from still unidentified sources, perhaps $\text{O}_2(\text{B}^3\Sigma)$. Current studies of climate change may therefore be inadequate about the role of stratospheric processes in tropospheric chemistry. These problems, detrimental to sound policy decision regarding N_2O and global change, should be addressed through the suggested research.

1. Introduction

Nitrous oxide (N_2O) is an important constituent of the atmosphere by virtue of its being the most important source of nitric oxide (NO) that destroys stratospheric O_3 and also a climatologically important greenhouse gas referred to in the Kyoto protocol for possible regulation (see <http://www.iisd.ca/climate/kyoto>). Sources and sinks of atmospheric N_2O are therefore matters of considerable importance. Until now it is commonly believed that there are no atmospheric photochemical sources of N_2O of any significance. This belief has been used in important global change and climate-chemistry studies (e.g., the Intergovernmental Panel on Climate Change (IPCC) initiated Third Assessment Report (TAR) entitled “Climate Change 2001” (see <http://www.ipcc.ch/activity/tar.htm>). Thus, models utilized for predicting climate changes have assumed that microbial activities at the Earth’s surface (soil, ocean) and anthropogenic activities are the only sources that need be considered and that atmospheric photochemical sources need not be included. In contrast, in recent years evidence for atmospheric production of N_2O from excited O_3 has been gaining strength from high quality laboratory experiments. Examination of atmospheric sources in the context of climate-chemistry and global change studies is therefore now timely and appropriate.

This paper starts with a review of laboratory experimental evidence for significant photochemical production of N_2O following electronic excitation of O_3 via absorption of Hartley-Huggins photons and from highly vibrationally excited ground state O_3 from O, O_2 recombination. These new sources of N_2O are then included in a two-dimensional coupled chemistry-radiation-transport atmospheric model. Results from this augmented atmospheric model are compared with observations of N_2O and CH_4 . This comparison suggests considerable model – observation differences in the case of N_2O in the stratosphere that seem to be mitigated

by inclusion of *in-situ* atmospheric production of N₂O from highly vibrationally excited O₃. It is, therefore, possible that assessments (like IPCC TAR) that predict climate change in the 21st century may have an inherent deficiency in their estimation of the stratospheric influence on the tropospheric chemistry. Equally importantly, tropospheric production of N₂O following the excitation of O₃ by the absorption of the Huggins band photons suggest that the actual microbial plus anthropogenic emission of N₂O needed to maintain the observed tropospheric N₂O is less than what one may expect in the absence of this production. Inverse modeling of N₂O, as practiced to date, may therefore have an intrinsic problem of inaccurately estimating the microbial and anthropogenic emission. These are detrimental to sound policy decisions with respect to possible regulation of N₂O as per the Kyoto protocol.

2. Foundation For Atmospheric Production of N₂O From Excited O₃

The case for atmospheric production of N₂O from excited O₃ rests on a solid foundation of much better measurements of N₂O quantum yields (ϕ_{N_2O}) by *Estupinan et al.* [2002] (henceforth ENLCW) and more powerful data analysis methods. These measurements of much higher accuracy (relative to previous measurement in the comparable pressure (p) and temperature (T) regime) were made using modern high-power laser flash photolysis and non-intrusive, highly sensitive, N₂O detection via tunable diode laser absorption spectroscopy (TDLAS). ϕ_{N_2O} were measured at 200 Torr \leq p \leq 800 Torr and 220K \leq T \leq 324K in UV photolysis of O₃/O₂/N₂ mixtures at 266 nm. Surprisingly, the ϕ_{N_2O} in this pressure regime was unmistakably greater (by a factor of almost ten at 1 atm and 295K) than the ϕ_{N_2O} due to O(¹D), N₂ association characterized by the p² dependence previously reported by *Kajimoto and Cvetanovic* [1975] (henceforth KC) at pressures ranging from 27 to 100 atmospheres.

Furthermore, the $\phi_{\text{N}_2\text{O}}$ in the low-pressure regime ($200 \text{ Torr} \leq p \leq 800 \text{ Torr}$) showed a predominant linear variation with pressure (p^1) at constant T, in sharp contrast with the p^2 variation observed at the higher pressures.

Initially, ENLCW proposed that the p^1 -dependent $\phi_{\text{N}_2\text{O}}$ was due to three-body N_2 , $\text{O}(^1\text{D})$ association. Subsequently, Gas Kinetics Data Evaluation Panels of NASA [*Sander et al.*, 2002] and IUPAC (International Union of Pure and Applied Chemistry) agreed with ENLCW proposal and endorsed ENCLW proposal for use in atmospheric modeling studies. (see, for example, http://www.iupac-kinetic.ch.cam.ac.uk/summary/IUPACsumm_web_latest.pdf).

However, these recommendation may be premature because other interpretations of ENLCW data are possible and more importantly there is no experimental evidence, as yet, for a direct link between $\text{O}(^1\text{D})$ and the measured linear-in- p $\phi_{\text{N}_2\text{O}}$. For example, there is no experimental information on how the deduced $\phi_{\text{N}_2\text{O}}$ is affected by the introduction of species that affect the $\text{O}(^1\text{D})$ concentration in the photolysis cell. Absence of this information is in significant contrast with the established O_2 -suppression of p^2 -dependent $\phi_{\text{N}_2\text{O}}$ in the high-pressure regime observed by KC. In fact, a meta-analysis of ENLCW's and KC's $\phi_{\text{N}_2\text{O}}$ in UV photolysis of O_3 -air [*Prasad*, 2002, 2005] suggests a new model of $\phi_{\text{N}_2\text{O}}$ that works smoothly over a wide p, T range (i.e., $200 \text{ Torr} \leq p \leq 110 \text{ atm}$ and $220\text{K} \leq T \leq 324\text{K}$). The unique features of this meta-analysis were the use of non-linear regression analysis and the use of the entire available data as one set. This approach enables extraction of smaller components that elude detection when the observed $\phi_{\text{N}_2\text{O}}$ are analyzed in small pieces (e.g., a set of only 4 to 5 $\phi_{\text{N}_2\text{O}}$ at a given T as was the case in ENLCW's study).

The new model of $\phi_{\text{N}_2\text{O}}$, which under atmospheric conditions is adequately represented by the equation (1) below, has three components.

$$\phi_{\text{N}_2\text{O}} = \mathcal{C} \exp(-\alpha/T) + m [M] + \beta [M]^2 (295/T)^\gamma \quad (1)$$

[M] in the equation (1) is the total number density, i.e., $[M] = [\text{N}_2] + [\text{O}_2]$. The values of the parameters, $\mathcal{C} = 5.630 \times 10^{-5}$, $\alpha = 1.899 \times 10^3$, $m = 5.452 \times 10^{-26}$ and $\beta = 4.386 \times 10^{-46}$, and $\gamma = 0.6$ are from the analysis of ENLCW's $\phi_{\text{N}_2\text{O}}$ done by *Prasad* [2005]. Note that one component of the model has a quadratic dependence on the total number density [M] (i.e., $[M]^2$ or p^2 at constant T). This component was attributed by KC to the three-body $\text{O}(^1\text{D})$, N_2 association. For photolysis in the Hartley band, the linear-in-[M] (or $[M]^1$) but T-independent component may be associated with the reaction (R1) below.



Alternatively, it may also be associated with a still unidentified species that is linearly connected with the $\text{O}_3(^1\text{B}_2)$ precursor and has an intrinsic lifetime much shorter than the collisional lifetime. Based upon *DeMore and Raper* [1962] experiment, N_2O production may also occur via the reaction (R1) when $\text{O}_3(^1\text{B}_2)$ reactant is replaced by the electronically excited singlet O_3 created by the absorption of Huggins band photon. In this case N_2O production would be wavelength dependent maximizing around 320 nm (see Figure 2 of *Prasad* [2002] and related discussions). To be fair, it must be stressed that the attribution of the $[M]^1$ -component to the reactions mentioned above also lacks direct experimental verification – just like the case with NASA and IUPAC recommendation. However, this does not affect the calculation of atmospheric production of N_2O corresponding to the $[M]^1$ -component. This will be obvious shortly.

The third, [M]-independent (i.e., $[M]^0$) but T-dependent component was initially attributed to reaction (R2).



For the reasons stated by *Prasad* [2005], the $[M]^0$ -component would be unimportant in atmospheric chemistry if it is due to the reaction of $O_3(^3B_1)$. Most recently, *Prasad and Zipf* [2006] pointed out that the $[M]^0$ -component might also be due to reactions of N_2 with highly vibrationally excited $O_3(X^1A_1)$, near the threshold of dissociation (henceforth $O_3^{N_2O}$ in shorthand notation). They also found some observational evidence for the N_2O production from $O_3^{N_2O}$. Next two sections describe the atmospheric model that was used to assess the implications of these sources of N_2O and the results of the improved modeling of the atmospheric N_2O distributions.

3. The Atmospheric Model

The atmospheric model used in the present study is our implementation of SOCRATES (Simulation of Chemistry, Radiation, and Transport of Environmentally important Species) that was originally developed at NCAR (National Center for Atmospheric Research) as community model. The generic SOCRATES model extends from $85^{\circ}S$ to $85^{\circ}N$ in latitude (in steps of 5°) and from ground to 120 km in 1 km steps. The generic model and the list of species and their reactions distributed with the model can be accessed at NCAR's Community Data Portal (CDP) (<https://cdp.ucar.edu/browse.do?uri=http://dataportal.ucar.edu/metadata/acd/software/software.thredds.xml>) after a simple registration. The generic model has been expanded to include advances in atmospheric chemistry since the time the SOCRATES development was frozen. The expansion is described in some detail in *Prasad and Zipf* [2004]. The expanded model has 192 reactions involving 53 species. For the present study the Prasad-Zipf implementation of SOCRATES was further elaborated by including atmospheric production of N_2O from excited O_3 as discussed in the previous section and additional computational details given below.

Furthermore, the original scheme of calculating the O(¹D) yield was replaced by the scheme recommended in JPL 02-25 [Sander et al., 2002]. The original O₃ absorption cross sections and their temperature dependence are now from Malicet et al. [1995] as recommended in JPL 02-25.

As per the equation 1, N₂O production rate via the [M]²-dependent component of ϕ_{N_2O} (the KC mechanism), hereafter p_{KC} , was calculated by equation (2) below.

$$p_{KC} = \sum_{\lambda} 4.386 \times 10^{-46} [M]^2 (295/T)^{0.6} J_{\lambda}(O_3) f_{\lambda}(O(^1D)) [O_3] \quad (2)$$

In the equation (2), $J_{\lambda}(O_3)$ is the photodissociation rate (s⁻¹) of O₃ at λ and $f_{\lambda}(O(^1D))$ is the yield of O(¹D) at that λ . The λ dependence of f_{λ} is exactly the same as that of the O(¹D) yield in UV photolysis of O₃ recommended in JPL02-25 [Sander et al., 2002]. However, the f_{λ} is normalized to unity at 266 nm. The summation extends over all those wavelength bins that span the UV in the SOCRATES model. The [M] and T are the atmospheric number density ([N₂] + [O₂]) and temperature where p_{KC} is being evaluated. Production of N₂O rate via the [M]¹-dependent component of ϕ_{N_2O} , hereinafter p_{HH} , was calculated by the equation (3) below.

$$p_{HH} = \sum_{\lambda} 5.452 \times 10^{-26} [M] J_{\lambda}(O_3) g_{\lambda} [O_3] \quad (3)$$

The g_{λ} in the equation (3) varies with λ across the Hartley-Huggins band such that $g_{\lambda} = 1$ in the Hartley band. It then decreases with λ for $\lambda > 300$ nm, but soon increases rapidly with λ in the Huggins band until $g_{\lambda} = 5.63$ at $\lambda = 320$ nm. After that, g_{λ} decreases slowly with λ such that $g_{\lambda} = 0$ at $\lambda \geq 360$ nm. It is worth mentioning here that the calculation of p_{HH} with the equation (3) is practically immune to the current controversy about what process may be actually responsible for the [M]¹-dependent component. This is so since the equation (3) is based solely on the experimental data of ENLCW and DeMore and Raper [1962], and very well known property of liquid nitrogen that one volume of liquid nitrogen expands to produce 696.5 equivalent volumes

of gas, as per the analysis of *Prasad* [2002]. Note that the λ -dependence is consistent with the increased lifetime of the excited O_3 responsible for the Huggins band.

Lastly, N_2O production rate via the $[M]^0$ -component, hereinafter $p_{O_3N_2O}$, was calculated by the equation (4) below.

$$p_{O_3N_2O} = 3.378 \times 10^{-38} \exp(-1899/T) (300./T)^{2.4} [O(^3P)] [O_2] [M] \quad (4)$$

Following *Prasad and Zipf* [2006], the equation (4) assumes that the $[M]^0$ -component is due to the $O_3^{N_2O}$. The numerical factor in the equation (4) is the product of \mathcal{C} of $\mathcal{C} \exp(-\alpha/T)$ of *Prasad* [2005] and the constant in rate coefficient for the $O(^3P)$, O_2 three-body recombination.

4. Modeling Runs, Results And Their Comparison With Observations

Three modeling runs (Model 0, Model 1 and Model 2) were made to assess the implications of atmospheric photochemical production of N_2O from excited O_3 . Model 0 assumed that atmospheric photochemical production of N_2O occurs via the KC mechanism only. In the Model 1, production from electronically excited O_3 (the $[M]^1$ -component of ϕ_{N_2O}) was added to the production from the KC mechanism. The production from $O_3^{N_2O}$ was added to the other two productions in the Model 2. All three models used specified volume mixing ratio (vmr), based on observations, as the lower boundary condition for N_2O . The fixed vmr was preferred over the flux as the lower boundary condition, since vmr is observationally known and since the flux at the lower boundary is the subject matter of investigation here. However, some model runs were made with flux as the lower boundary condition, as will be explained later. Models were run for 60 years. This was judged sufficient since the starting N_2O was already close to the solution and because of it there was indeed hardly any change after 45 years.

4.1 N₂O Production Rates

Altitude profiles of globally averaged N₂O production rates from the KC mechanism (O(¹D), N₂ association), electronically excited O₃ and O₃^{N₂O} for the months of July (top part) and October (bottom part) are shown in the figure 1. The production from electronically excited O₃ predominates in the troposphere and the lower stratosphere. Most of production from electronically excited O₃ is due to the O₃ excited by the absorption of the Huggins band photon. This is due to deep penetration of these photons and the higher g_{λ} in this band. Contribution of the O₃ excited by the absorption of Hartley band is much smaller due to both the lower [N₂] where Hartley band is absorbed and the lower g_{λ} . At about 35 km, the production from O₃^{N₂O} crosses over the production from the electronically excited O₃. Note that the contribution of O-atoms from photodissociation of O₂ in this region is automatically included through the use of the equation (3). Also note that this contribution is also the reason why the N₂O production remains significant where the contributions of the other two components becomes negligible. The globally averaged production rates for the two months (July and October) have very similar profiles, despite very different sun's position during these months. It should, however, be noted that while the global averaging makes the production rate profiles look similar there are considerable differences at the regional scale defined by latitudes. For example, there is no production in the dark southern high latitudes during July in contrast with the considerable production in the sunlit northern high latitudes. These and other differences in the N₂O production rates during very different solar conditions of July and October can be appreciated from the contour plots shown in the Figure 2.

4.2 N₂O Volume Mixing Ratios in the Three Models

Figure 3 presents the globally averaged N₂O volume mixing ratios (vmr) for the three models for July (northern hemispheric summer). The results for other seasons are very similar. If the production from O₃^{N₂O} is neglected then there is hardly any difference in the N₂O vmr even up to 60 km. Even with the production from O₃^{N₂O} included (i.e., Model 2), the vmr for the three models are practically the same up to about 35 km. The effects of N₂O production from O₃^{N₂O} on the modeled vmr begins to manifest at the higher altitudes.

A more detailed quantitative information emerges from two latitudinally resolved views, shown in contour plots presented in the Fig 4, one for the lower altitudes 0 to 30 km (the bottom part) and the other for the higher 30 to 60 km (the top part). Both contour plots are for the percent differences in the vmr calculated in the two cases of no N₂O production from any form of excited O₃ (Model 0) and the case with production from only electronically excited O₃ (Model 1). At higher latitudes (> 40°), a very small difference (0.02%) begins to emerge at about 10 km and steadily grows with altitude. At the lower latitudes, that small difference starts to show up at higher altitudes between 15 to 20 km, depending upon the latitudes. Differences between the modeled vmr, with respect to both altitude range coverage and magnitude, maximize in the sunlit summer high latitude region. These differences, seen in the top part of Figure 4, are consistent with the contour plots of N₂O production rates in July presented in the Figure 2 (top part).

Despite their being less than 0.02% at about 10 km and their decreasing to zero at the lower boundary (due to the imposed boundary condition), the differences between the vmr for the Model 0 and Model 1 are significant. The introduction of the tropospheric production of N₂O (maximizing in the lowest troposphere) causes the concentration gradient to be less steep in the Model 1 relative to that in the Model 0. Thus, the effect of tropospheric production of N₂O from

electronically excited O_3 shows up in the amount of surface fluxes implied by the three models 0, 1 and 2. This flux and its global average can be estimated in several ways. For example, ignoring the small N_2O growth, the global average flux is just the difference between the globally averaged atmospheric production and loss rates, i.e., net loss. These fluxes can also be calculated from the known vertical diffusion coefficients and the modeled gradients in N_2O concentration at the two lowest altitudes, say 0 and 1 km. The global average can then be calculated by taking the global average of the vertical fluxes calculated for the various latitude bins of the model. Both methods have their advantages and disadvantages. The first is an integral method and should therefore be more accurate than the second method that involves differential of concentrations that show only very small gradient near the surface. Another difficulty with the second method is that it would give the flux through a surface at 0.5 km (if 0 and 1 km concentrations are used to calculate the concentration gradient). However, this is not real concern since in the absence of loss the flux through the layer at 0.5 km would for all practical purpose the same as the surface emission. Similarly, the first method has the disadvantage that the globally averaged net loss would equal the globally averaged surface flux only when the growth of N_2O with time is neglected. Nevertheless, quite the same conclusion is arrived at, no matter which method is used. Figure 5 shows the estimated flux from the first method. It is seen that with N_2O production from electronically O_3 included in the model (i.e., Model 1) about 7% less surface flux maintains the observed tropospheric N_2O vmr, compared to the case of a model that excludes this production (i.e., Model 0). This was verified by the two additional modeling runs, both using specified flux condition at the lower boundary instead of specified vmr. In one case the N_2O production from excited O_3 was neglected while in the other it was included. Higher N_2O was predicted in the second case verifying the point we are making. Lesser surface

flux would suffice if the production of N₂O via the potential reaction $O_3(^3A_2) + N_2 \rightarrow N_2O + O_2$ [Prasad, 1997] occurs. Note that unlike $O_3(^3B_1)$, which is atmospherically unimportant due to the $O_3(^3B_1) \leftarrow O_3(X^1A_1)$ transition being optically forbidden, the optical excitation of $O_3(^3A_2)$ via $O_3(^3A_2) \leftarrow O_3(X^1A_1)$ transition becomes allowed and the lowest lying triplet $O_3(^3A_2)$ can be significantly excited by absorption of solar radiation (see Prasad [1997] for some more specifics of excitation rates).

Addition of the N₂O production from $O_3^{N_2O}$ (in the Model 2) has no effect on the needed surface flux (although as will see in the next section that the production from $O_3^{N_2O}$ has a significant effect on the N₂O vmr at the higher altitudes). Hardly any difference in the surface fluxes estimated for Models 1 and 2 is easily explicable, because the column integrated N₂O production from $O_3^{N_2O}$ is much smaller than the same from electronically excited O₃.

4.2.1 A Potentially Important Implication For Global Change Studies

In the context of global warming or global change studies, considerable efforts are being directed towards building, as accurate as possible, source-sink budget of greenhouse gases included in the Kyoto Protocol. As a result, a global gridded inventory has been compiled that represents the current understanding of geographical distribution of surface sources of N₂O [Bouwman *et al.*, 1995]. Nevertheless, as emphasized by Bouwman and Taylor [1996], the source strengths and the seasonality of the surface sources and sinks remain uncertain. Because of this, attempts have been made to reduce those uncertainties through complementary inverse modeling techniques [Prinn *et al.*, 1990; Hirsch *et al.*, 2006].

For inverse modeling of N₂O to achieve its stated goal, it must account for (as accurately as possible) all N₂O related atmospheric photochemical processes. For example, and as emphasized by Hirsch *et al.* [2006], neglect (or even inaccurate accounting) of the

photochemical loss of N₂O would introduce spurious component to the surface flux signal. From the same token, neglect of photochemical production of N₂O from various forms of excited O₃ (for which evidences have been discussed in this paper) would also introduce spurious components to the surface emissions. Based on the data in the Figure 5, the magnitude of the so introduced spurious element could potentially approach about 7% for the globally averaged surface emission. It may, conditionally, even exceed 7% as explained earlier.

From the above discussion, previous inverse modeling estimates of the microbial and anthropogenic fluxes, in either the various “super regions” or the various latitudinal regions, may not be as correct as they should be, since those inverse modeling have neglected atmospheric production of N₂O from excited O₃. Since the tropospheric N₂O production from electronically excited O₃ has a distinct seasonality (see Figure 2), the seasonality of the surface sources of N₂O estimated from the previous inverse modeling is also at risk. The risk level in the seasonality of the N₂O surface flux derived for the various regions (including the “super regions”) would be greater than the risk level ($\geq 7\%$ error) for the globally surface averaged flux. This situation should be corrected to ensure as accurate as possible N₂O source-sink inventory for climate or global change predictions.

4.2.2 Why It Matters?

While neglect of tropospheric production of N₂O from excited O₃ may be tolerable in modeling the present atmosphere (since N₂O is an observed constituent), that neglect can put forecasting of global change at risk. This is so since surface emission and the tropospheric production of N₂O differ in the causes and rates of their growth. The two components of the atmospheric N₂O would contribute to the N₂O growth rate at different rate and due to different

causes. The predictions of N₂O in future atmosphere could lose reliability if the two contributing factors to N₂O growth are not carefully distinguished.

4.3 Comparison With Observations

4.3.1 The Observational Data

The observational data used in this study are the observations of N₂O and CH₄ made by the CLAES (Cryogenic Limb Array Etalon Sounder) instrument [Roche *et al.*, 1996] on board the UARS (Upper Atmospheric Research Satellite) satellite. Measurements of N₂O are also available from the ATMOS (Atmospheric Trace Molecule Spectroscopy) instrument on board the Space Shuttle [Gunson *et al.*, 1990] and from SAMS (Stratosphere and Mesosphere Sounder) instrument on board Nimbus-7 [Jones and Pyle, 1984]). However, because of its relatively larger global coverage in both space and time, we have used only the CLAES data. This database has been used in many studies. W. J. Randel, in particular, has used the CLAES data to create a climatology of N₂O and CH₄, comprising of monthly mean N₂O and CH₄ vmr for twelve months at sixteen pressure levels and forty-one latitude bins ranging from 80°S to 80°N in 4° wide bins. The pressure levels used in this climatology are: 100, 68.13, 46.42, 31.63, 21.54, 14.68, 10.00, 6.81, 4.64, 3.16, 2.15, 1.47, 1.00, 0.68, 0.46, 0.32 mb. The database is available from SPARC Data Center Website: <http://www.sparc.sunysb.edu/html/RefData.html>.

4.3.2 Highlights of Comparison With Observations

Our model-observation comparison suggests a N₂O source-deficit problem. Since the problem seems to be only slightly alleviated by inclusion of the N₂O production from O₃^{N₂O}, a missing N₂O sources in the stratosphere is indicated. These points can be appreciated from the following figures. To start with, Figure 6 presents the globally averaged modeled and observed altitude profiles N₂O and CH₄ vmr for July, in respectively the top and bottom part. We chose to

use global averages of the modeled vmr to illustrate our point since this averaging minimizes error due to uncertainties in model dynamics, (e.g., the inability of the two-dimensional models to reproduce the observed double peaks in the latitudinal distributions of both N₂O and CH₄). The stated example of model deficiency is also the reason for starting with the month of July when there are no double peaks. It is recognized that even after global averaging there is a residual uncertainty due to uncertainty in the vertical eddy diffusion coefficient (k_{zz}). It will, however, be soon obvious that the uncertainty in k_{zz} may not negate the inference about N₂O source-deficit.

From the Figure 6, it is obvious that while the modeled CH₄ vmr are close to the observed, models underestimate N₂O in the stratosphere. Assuming that the currently known atmospheric CH₄ photochemistry has no major flaws (and there is no reason to assume otherwise), the extent of model-observation disagreement attributable to deficiencies in model dynamics can be taken to be what we see in the case of CH₄. Thus, the much larger model-observation disagreement in the case of N₂O is logically attributable to still missing atmospheric photochemical sources. This thesis is supported by the fact that addition of N₂O production from O₃^{N₂O} seems to bring about non-negligible improvement.

For a better comprehension of the extent of the N₂O source deficiency, Figures 7 (for January) and 8 (for October) present the globally averaged modeled-vmr/observed-vmr ratios for both N₂O and CH₄ for the three models as a function of the pressure levels. These months have been selected to underscore the fact that model-observations disagreements discussed in the previous paragraphs are not limited to July only. At each pressure level, the globally averaged absolute value of the deviation of each ratio in any given latitude band from the globally averaged ratio was also calculated and attached to the ratios as an error bar. For the purpose of

preparing these figures, Randel's climatology database was regridded on the 5° -wide latitude bins used in SOCRATES, and the modeled vmr were regridded from SOCRATES pressure levels to pressure levels used in Randel's climatology. Furthermore, in contrast with previous figures, the profiles of the ratios span only those pressure-levels (altitudes) for which extensive observations of N_2O and CH_4 are available from CLAES.

It is clearly seen that the globally averaged modeled/observed vmr ratios for CH_4 remains within 0.8 to 1.16 (or 16 to 20% of the ideal value of 1) in both Figures 7 and 8 covering very different seasonal conditions. Even after adjusting for the globally averaged deviation from the mean, the adjusted global mean values are also not too far from the ideal value. For example, they are 0.7 at the most on the low side and 1.38 on the high side in the Figure 7. As expected, this behavior is independent of which model (0, 1 or 2) is considered. The deviation from the ideal value is due to combination of observational errors and imperfection of model dynamics.

In case of N_2O , however, a very different situation is encountered. The values resemble the CH_4 only up to 10 mb. At lower pressure levels (higher altitude) the global mean values steadily decrease from 1 at about 10 mb to 0.2 at the 0.32 mb in the case of Model 0 and 1. Even after adjustment for the deviation from the mean, the adjusted global mean values are much less than the ideal value near unity, e.g., 0.3 at the 0.32 mb in both Figures 7 and 8. Judging from the case of CH_4 , this sharp decrease from 1 to 0.2 may not be due to observational errors and/or model transport deficiency. It seems more logical to attribute this to chemistry, particularly, source deficit in the model. This attribution is supported by the fact that inclusion of the N_2O production from $\text{O}_3^{\text{N}_2\text{O}}$ leads to substantive improvement at the higher altitudes. For example, at the 0.32 mb, the value of the ratio increases from about 0.2 to about 0.4 in the Model 2, that is well above the best possible global mean value in the Models 0 and 1.

The situation that even with the inclusion of N₂O production from O₃^{N₂O} there is still substantial underprediction of N₂O vmr in the above the 10 mb level, suggests that there are still missing sources of N₂O in this region. One could conjecture about systematic over-measurement of N₂O by CLAES at higher altitudes. However, there is no reason at the present to entertain such a conjecture. Source deficiency in the models seems to a better explanation for the problem with the atmospheric N₂O models seen in the Figures 7 and 8.

4.3.3 A Perspective on Previous Model-Observation Comparison

The idea of N₂O source deficit now, after decades of atmospheric N₂O related studies, might appear ironic. However, there need not be any irony. Model-observations, prior to the CLAES/UARS era, could not have detected the possibility of missing sources in the upper stratosphere, due to lack of extensive global measurement of N₂O in that region. In the post-CLAES/UARS era, on the other hand, the emphasis was on latitudinally resolved comparisons to validate three-dimensional CTM (Chemistry Transport Model), correlation of N₂O with other tracer molecules, vortex processes (e.g., Rasch *et al.*, 1997, Waugh *et al.*, 1997; Douglass *et al.*, 1999; Olsen *et al.*, 2001]).

Douglass et al. [1999] study, for example, was in the context of choosing meteorological inputs from CCM2, GISS II and GEOS-DAS for Global Modeling Initiative (GMI) assessment of high-speed aircraft. (In the GMI context, CCM2 is the three-dimensional middle atmospheric version of the Community Climate Model from NCAR. GISS II is the GCM (General Circulation Model) from Goddard Institute for Space Studies (GISS). GEOS-DAS is Goddard Earth Observing System Data Assimilation System. Overestimation of the N₂O in the lower stratosphere by all of the three meteorological inputs used in the GMI assessment agrees with our results (i.e., $1.0 \leq \text{model/observation ratio} \leq 1.2$ for N₂O in the region with $p > 10$ mb in both

Figures 7 and 8). For the upper stratosphere, however, there were considerable latitude-dependent differences from one dynamical-input to another in the GMI assessment. Near the equator (5N to 5S), for example, while the GEOS-DAS input best represented the CLAES N₂O data in both magnitude and profile-shape, the GISS and CCM2 both underestimated the CLAES N₂O profile. In contrast, in 40⁰ to 50⁰ latitude bins in both the northern and southern hemisphere both CCM2 and GISS agree very well with CLAES observation while GEOS-DAS overestimates the N₂O. In an earlier study, *Rasch et al.* [1995], compared the modeled vmr of N₂O from middle atmospheric version 2 of CCM (aka MACCM2) with the N₂O measurements from both ATMOS and SAMS. They found that the model had underestimated the N₂O with measurements by both instruments at 48⁰ S and 28⁰ N in the region above 30 km. Also, while being in good agreement at 2⁰N in March, the model underestimated ISAMS measurement of N₂O at 40⁰ N at altitudes above 30 km.

A later study of the N₂O – NO_y [*Olsen et al.*, 2001] also found a similar underestimation of the stratospheric N₂O in three dimensional framework. These authors compared N₂O measurements by the ATMOS and predictions of N₂O distributions by the University of California Irvine (UCI) three-dimensional CTM using three meteorological fields (Met-fields). The three Met-fields were taken from the archived outputs of the GISS GCM labeled as GISS-II, GISS-II' 31L and GISS-II' 23L. Compared to GISS II, both GISS-II' models had a better latitude-longitude resolution. When the Met-field generated by the better GISS II' models was used in the CTM, the modeled N₂O was clearly less (by as much as 50 ppb) in the middle to upper stratosphere in the 10⁰ N and S latitude bin. There were better agreements at 40⁰ to 50⁰ for which they present their comparison.

Consistent with these snapshot comparisons, at various latitude-bins, in previous studies, considerable, latitudinal variations are seen in the present study also. In fact, the possibility that latitudinal difference might cloud the global picture was the additional reason why comparison with observations was made for globally averaged profiles. Unfortunately, in the absence of the globally averaged information in the previous studies, it is very difficult to say anything more specific about how the N₂O source-deficit found in this study stands in relation to previous studies. Furthermore, the N₂O profile in the upper stratosphere is very sensitive to the N₂O photodissociation that is related to the temperature dependent absorption cross-sections. Thus, in comparing the results from CTM with the present results, it is noteworthy that in the three-dimensional model the photodissociation rates are usually determined by interpolations from a pre-calculated table prepared at a coarse time resolution, i.e., monthly mean and diurnally averaged [Olsen *et al.* 2001]. In contrast, the calculations of the photodissociation rate in SOCRATES are more direct and at much better time resolution (i.e., every five days and at eight time steps in twenty-four hours). Because the modeled N₂O vmr is also dependent upon the N₂O + O(¹D) → product reaction and through it on the modeled O(¹D) vmr, it should be further emphasized that the present study uses O(¹D) quantum yield in UV photolysis of O₃ from Sander *et al.* [2002] and O₃ absorption cross sections from Malicet *et al.* [1995] as per JPL 02-005 recommendation. These add to the difficulties of comparing the results of the present study with those of previous studies. Partly for this reason and because of the important implications of the missing sources of N₂O (discussed in the next subsection), the best course of action at the present stage should be to pursue, rather than ignore, the missing source suggested by the present study. Needed modeling and laboratory studies are discussed in the Section 5.

4.3.4 Potentially Important Implication of The Missing Source in Global Change Studies

The tropospheric chemistry is directly affected by stratospheric processes, including the stratospheric O₃ [Prather and Ehhalt, 2001]. One obvious example is the flux of NO_x and O₃ rich stratospheric air into the troposphere through the fold in the tropopause (i.e., the stratospheric-tropospheric exchange process). Stratospheric O₃ and NO_x both are significantly influenced by stratospheric N₂O. Because of this, missing sources of N₂O in the upper stratosphere implied by the present study poses a risk that models currently used for global change studies could potentially miscalculate the influence of stratospheric processes on the tropospheric chemistry and thereby on climate change. This is a matter of concern. Fortunately, further modeling and laboratory research such as those described in the next section can easily mitigate the concern.

5. Suggestion For Future Modeling and Laboratory Studies

5.1 Extension of The Present Modeling

The present study should be repeated with three objectives, not necessarily in the stated order. First, is further exploration of the intriguing N₂O-deficit problem in the region above 10 mb even after the inclusion of N₂O production from excited O₃. This needs consideration of those proposed sources of N₂O that may become important in that region. Olsen *et al.* [2001] have explored this area. They did a modeling experiment with the reaction of excited NO₂ (\tilde{A}^2B_1 , 2B_2) with N₂. This reaction was originally proposed by Zellner *et al.* [1992]. Unfortunately, this reaction was doubtful from the very beginning. From many studies, the exothermic reverse reaction $N_2O + NO \rightarrow NO_2 + N_2$ has a high activation energy of about 50 kcal mole⁻¹ (see, for example, Fisburne and Edse, [1964]). As a corollary, the $NO_2 + N_2 \rightarrow N_2O + NO$ reaction

should have a barrier of about 83 kcal mole⁻¹, if the reversibility of reaction is assumed to hold. Obviously, the electronic energy in NO₂ (\tilde{A}^2B_1 , 2B_2) is too little to overcome the expected barrier. Consistent with this doubt, more sensitive laboratory studies of *Estupinan et al.* [2001] has now decisively shown that the reaction NO₂ (\tilde{A}^2B_1 , 2B_2) + N₂ → N₂O + NO is so very slow that the production of N₂O from excited NO₂ (\tilde{A}^2B_1 , 2B_2) is of no consequence in atmospheric chemistry. It is therefore important to try other sources of N₂O, such the reaction O₂(B³Σ) + N₂ → N₂O + O [Prasad and Zipf, 2002]. This spin conserving simple reaction is expected to be significantly faster than the Woodward-Hoffman forbidden O₂(B³Σ) + N₂ → NO + NO (or, N + NO₂) reaction studied by Zipf and Prasad [1998]. Thus, from the altitude profiles of NO (or NO₂) production from the O₂(B³Σ) + N₂ → NO + NO (or, N + NO₂) reaction presented by Prasad and Zipf [2004], it is easily seen that the production of N₂O from the O₂(B³Σ) + N₂ → N₂O + O reaction is considerable in the region of N₂O-source deficiency.

Second, is the use of more data from more recent observing missions, e.g., MLS [*Waters et al.* 2006] and HIRDLS [*Gille et al.*, 1994] instruments on board AURA Atmospheric Chemistry Mission, and the high latitude measurements of from ILAS [*Kanzawa et al.* 2003]. Third, these studies should preferably use other dynamical transport fields, for example, mean residual circulation derived from NCEP2 and/or archived dynamical outputs of three-dimensional model such as the Whole Air Community Climate Model (WACCM). This has been done recently by *Jiang et al.* [2004] and *Liang and Yung* [Preprint, entitled “Sources of the Oxygen Isotopic Anomaly in Atmospheric N₂O”, Mao-Chang Liang and Yuk L. Yung, submitted to *J. Geophys. Res.*, 2006]. This may enable meaningful comparisons in various latitude bins also. Equally importantly, the suggested new modeling studies should examine not only the comparison between the predicted and observed N₂O, but also the comparison between

the modeled and observed correlation between N_2O and other species such as NO_y . *Olsen et al.* [2001] found that a stratospheric source of N_2O should be verifiable through comparison between the predicted and observed $\text{NO}_y/\text{N}_2\text{O}$ correlation. However, their N_2O source was dependent upon NO_x (i.e., NO_2). Whether the same would be true if the N_2O source is derived not from NO_x but from O_3 and O_2 needs to be checked.

5.2 Inverse Modeling

Given the importance of as accurate as possible source-sink inventory of greenhouse gases included in Kyoto Protocols, inverse modeling of N_2O should be improved by including tropospheric production of N_2O from electronically excited O_3 . This improvement need not wait for the laboratory studies discussed in the next subsection. In due course, the results of further experiments will add extra refinements to inverse modeling.

5.3 Laboratory Studies

The first priority in future laboratory studies should be on the study of $\phi_{\text{N}_2\text{O}}$ in UV photolysis of O_3 -air mixture in gas phase by Huggins band photons around 320 nm and on a more accurate determination of the N_2O yield from $\text{O}_3^{\text{N}_2\text{O}}$. The desirable approach for these experiments have been already discussed [*Prasad*, 2002; *Prasad and Zipf*, 2006]. Next, and as soon as the suggested extension of the present modeling identifies the mechanism capable of removing the N_2O -deficit problem, the laboratory studies should look at that mechanism.

Acknowledgement.

One of us (SSP) acknowledges the support of the NASA grant NNG04GL29G.

References

Bouwman, A. F., K. W. Van der Hoek, and J. G. J. Olivier (1995), Uncertainties in the global source distribution of nitrous oxide, *J. Geophys. Res.*, *100*(D2), 2785–2800.

Bouwman, A. F., and J. A. Taylor (1996), Testing high-resolution nitrous oxide emission estimates against observations using an atmospheric transport model, *Global Biogeochem. Cycles*, *10*(2), 307–318.

DeMore, W. B. and O. F. Raper (1962), Reactions of O(¹D) with N₂, *J. Chem. Phys.*, *37*, 2048.

Douglass, A. R. ; Prather, M. J. ; Hall, T. M. ; Strahan, S. E. ; Rasch, P. J. ; Sparling, L. C. ; Coy, L. ; Rodriguez, J. M. (1999), Choosing meteorological input for the global modeling initiative assessment of high-speed aircraft *J. Geophys. Res.* *104*(D22) , 27,545 – 27,564.

Estupiñán, E.G. , J.M. Nicovich, J. Li, D. M. Cunnold, P.H.Wine (2002), Investigation of N₂O production from 266 and 532 nm laser flash photolysis of O₃/N₂/O₂ mixtures, *J. Phys. Chem. A* *106*, 5880-5890.

Estupiñán, E.G., R. E. Stickel, and P. H. Wine (2001), *Chem Phys. Lett.*, *336*, 109.

Fisburne, E. S., and R. Edse (1964), *J. Chem. Phys.*, *41*, 1297-1304.

Gille, J., J. Barnett, M. Coffey, W. Mankin, B. Johnson, M. Dials, J. Whitney, D. Woodard, P. Arter, and W. Rudolf (1994), The High Resolution Dynamics Limb Sounder (HIRDLS) for the Earth Observing System SPIE, 2266, 330-339.

Gunson, M. R., C. B. Farmer, R. H. Norton, R. Zander, C. P. Rinsland, J. H. Shaw, and B. C. Gao, (1990), Measurements of CH₄, N₂O, CO, H₂O, and O₃ in the middle atmosphere by the ATMOS experiment on Spacelab 3, *J. Geophys. Res.*, 95, 13867-13882.

Hirsch, A. I., A. M. Michalak, L. M. Bruhwiler, W. Peters, E. J. Dlugokencky, and P. P. Tans (2006), Inverse modeling estimates of the global nitrous oxide surface flux from 1998–2001, *Global Biogeochem. Cycles*, 20, GB1008, doi:10.1029/2004GB002443.

Jiang, X., C. D. Camp, R. Shia, D. Noone, C. Walker, and Y. L. Yung (2004), Quasi-biennial oscillation and quasi-biennial oscillation–annual beat in the tropical total column ozone: A two-dimensional model simulation, *J. Geophys. Res.*, 109, D16305, doi:10.1029/2003JD004377.

Jones, R. L., and J. A. Pyle (1984) Observations of CH₄ and N₂O by Nimbus 7 SAMS: A comparison of insitu data and two-dimensional numerical model calculations, *J. Geophys. Res.*, 89, 5263-5279.

Kajimoto, O, and R.J. Cvetanovic (1975) Formation of nitrous oxide in reactions of O(¹D₂) atom with nitrogen, *J. Chem. Phys.*, 64, 1005.

Kanzawa, H., *et al.* (2003), Validation and data characteristics of nitrous oxide and methane profiles observed by the Improved Limb Atmospheric Spectrometer (ILAS) and processed with the Version 5.20 algorithm, *J. Geophys. Res.*, *108*, D16, 8003, 10.1029/2002JD002458.

Malicet, J., D. Daumont, J. Charbonnier, C. Parisse, A. Chakir, and J. Brion (1995), Ozone UV spectroscopy: II. Absorption cross-sections and temperature dependence, *J. Atmos. Chem.*, *21*, 263–273, 1995.

Olsen, S. C. McLinden, C. A., and M. J. Prather (2001), Stratospheric N₂O - NO_y system: Testing uncertainties in three-dimensional framework, *J. Geophys. Res.*, *106*, 28,771-28,784.

Prasad, S. S. (1997), Potential atmospheric sources and sinks of nitrous oxide, 2, Possibilities from excited O₂, "embryonic" O₃, and optically pumped excited O₃, *J. Geophys. Res.*, *102*, 21,527-21,536.

Prasad, S. S. (2002), A new model of N₂O quantum yield in UV photolysis of O₃/O₂/N₂ mixtures: Contributions of electronically excited O₃ and O₃• N₂, *J. Chem. Phys.*, *117*, 10,104-10,108.

Prasad, S. S. (2005), Especially significant new component of N₂O quantum yield in the UV photolysis of O₃ in air, *J. Phys. Chem.*, *109*, 9035-9043.

Prasad, S. S., and E. C. Zipf (2000), Middle atmospheric sources of nitrous oxide (N_2O): $\text{O}_2(\text{B})$ and $\text{N}_2(\text{A})$ chemistry, *Phys. Chem. Earth (C)*, 25, 213-222.

Prasad, S. S., and E. C. Zipf (2004), Photochemical production of odd nitrogen directly from O_2 , N_2 principals: Atmospheric implications and related open issues, *J. Geophys. Res.*, 109, D08310, doi:10.1029/2003JD004061.

Prasad, S. S., and E. C. Zipf (2006) Especially Significant New Component of N_2O Quantum Yield in the UV Photolysis of O_3 in Air II: A Sequel Concerning the Role of $\text{O}_3(\text{X } ^1\text{A}_1, \text{high } \nu)$, submitted to *J. Phys. Chem.*

Prather, M., and D. Ehhalt, (2001), Chapter 4. Atmospheric Chemistry and Greenhouse Gases, in “Climate Change 2001: The Scientific Basis”, pp. 239– 287, edited by J. T. Houghton et al., Cambridge U. Press, Cambridge, 2001.

Prinn, R., D. Cunnold, R. Rasmussen, P. Simmonds, F. Alyea, A. Crawford, P. Fraser, and R. Rosen (1990), Atmospheric emissions and trends of nitrous oxide deduced from 10 years of ALE-GAGE data, *J. Geophys. Res.*, 95(D11), 18,369– 18,385.

Rasch, P. J., B. A. Boville, and G. P. Brasseur (1995) A three-dimensional general circulation model with coupled chemistry for the middle atmosphere, *J. Geophys. Res.*, 100, 9041-9072.

Roche *et al.* (1996), Validation of CH₄ and N₂O measurements by the cryogenic limb array etalon spectrometer instrument on the Upper Atmosphere Research Satellite, *J. Geophys. Res. Vol. 101 , No. D6 , p. 9679-9710 (95JD03442)*

Sander, S. P., et al, (2002), Chemical Kinetics and Photochemical Data for Use in Stratospheric Modeling, Evaluation No. 14, NASA JPL Publication 02-25, 2002

Waters, J.W., et al., (2006), The Earth Observing System Microwave Limb Sounder (EOS MLS) on the Aura satellite," *IEEE Trans. Geosci. Remote Sensing 44*, no. 5, 1075-1092.

Waugh, D. W. et al., (1997), Three-dimensional simulations of long-lived tracers using winds from MACCM2 , *J. Geophys. Res, 102 , 21,493-21,513.*

Zellner, R., D. Hartman, and I. Rosner (1992), N₂O formation in reactive collisional quenching of NO₃* and NO₂* by N₂, *Ber. Bunsenges. Phys. Chem., 96*, 385-390.

Zipf, E. C., and S. S. Prasad (1998), Evidence for new sources of NO_x in the lower atmosphere, *Science, 279*, 211-213.

Figure Captions

Figure 1. Altitude profiles of globally averaged N₂O production rates for the months of July (top part) and October (the bottom part). In each case, production rates are shown for the O(¹D), N₂ association as formulated by Kajimoto and Cvetanovic (KC), vibrationally highly excited ground state O₃ (O₃^{N₂O}) and electronically excited O₃ created by the absorption of the Hartley-Huggins band photons. These are identified by symbols described in the legend.

Figure 2. Contour plots of N₂O production rates from O₃^{N₂O} and from electronically excited O₃ for the months of July (top part) and October (bottom part). These are designed to reveal the latitudinal differences in the production rates as the season changes from summer/winter to fall/spring.

Figure 3. Globally averaged N₂O volume mixing ratios (vmr) for northern hemispheric summer (July). Results are shown for three models, Model 0, 1 and 2, that differ in only the assumption made about N₂O production. Model 0 assumed that there is no atmospheric production of N₂O from process other than the O(¹D), N₂ association formulated by KC. In Model 1, production from only electronically excited is also included. Model 2 additionally includes production from O₃^{N₂O}.

Figure 4. Contour plots of the difference between the N₂O vmr for the Model 1 and the Model 0, expressed as percentage of the Model 0 vmr. The top part of the plot covers the region from 30 to

60 km while the bottom part covers the region from 0 to 30 km. This bifurcation is designed to show the special features of the low and the higher altitude regions.

Figure 5. Bar plot of the surface flux of N₂O attributable to microbial and anthropogenic activities corresponding to Models 0, 1 and 2.

Figure 6. Plots of the vertical profiles of globally averaged modeled and observed N₂O vmr (the top part) and CH₄ (the bottom part) for July. Three modeled profiles correspond to Models 0, 1 and 2. The observed data are global average of the climatology constructed by W. J. Randel from UARS observations. Note that while the observed CH₄ vmr lie close to the modeled vmr throughout the atmospheric region covered by the figure, for N₂O the model-observation agreement is limited to the lower atmospheric region only. In the region above about 10 mb the modeled N₂O vmr are increasingly smaller than the observed.

Figure 7. Plots of the vertical profiles of the globally averaged modeled/observed vmr ratios for N₂O (the top part) and CH₄ (the bottom part) for July. Use of the ratio is designed to show the model-observation agreements/disagreement in more easily discernable quantitative form for each of the three models. The globally averaged values of the absolute values of the deviations of the ratios at a latitude bin from the global average mean ratio are also shown in the form of horizontal bars attached to global mean values. Note that the figures show a N₂O source deficit problem in the stratosphere.

Figure 8. The same as the Figure 7, except it is for the month of October (or fall/spring).

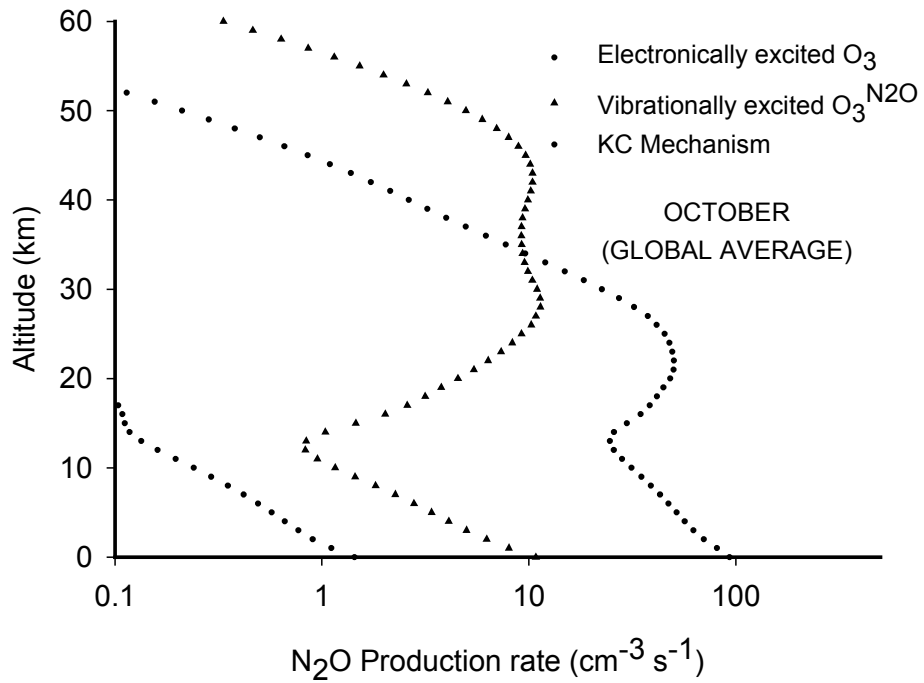
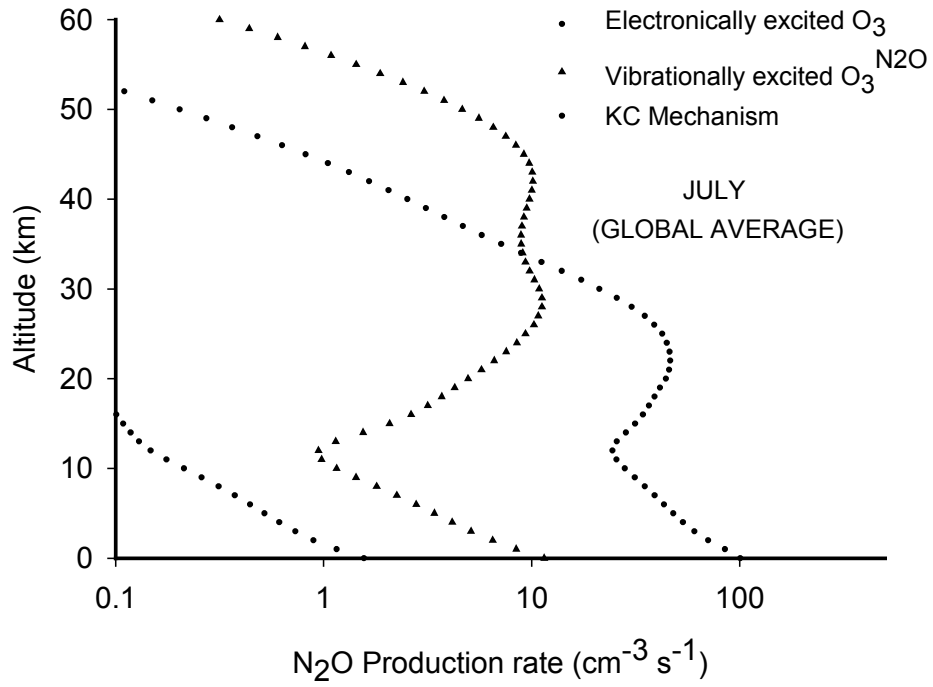


Figure 1

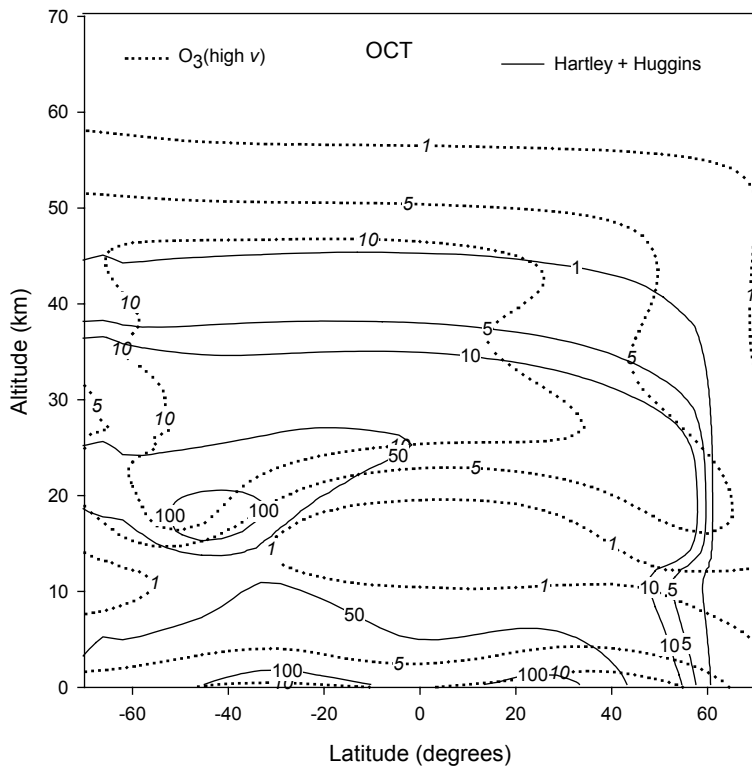
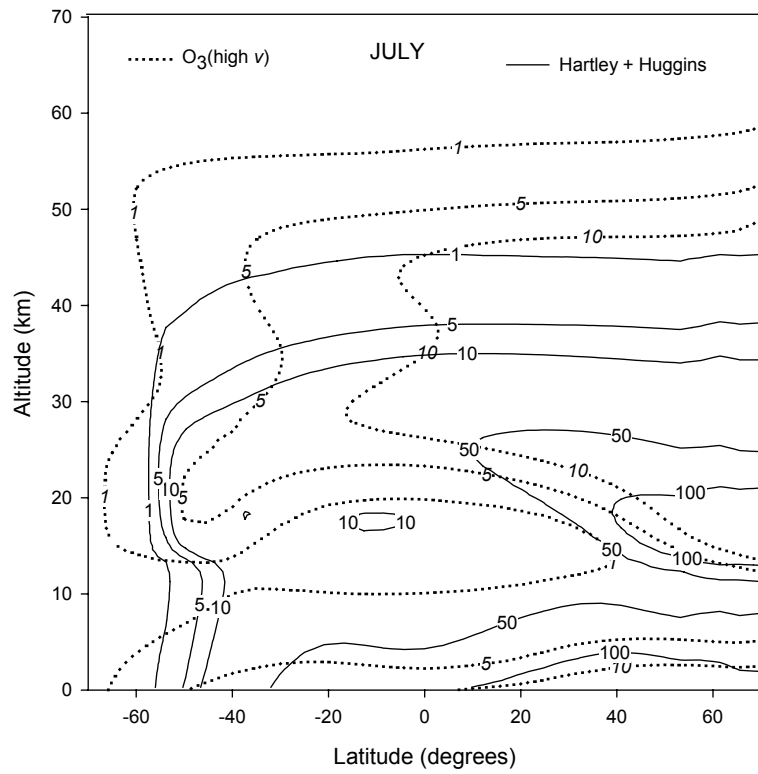


Figure 2

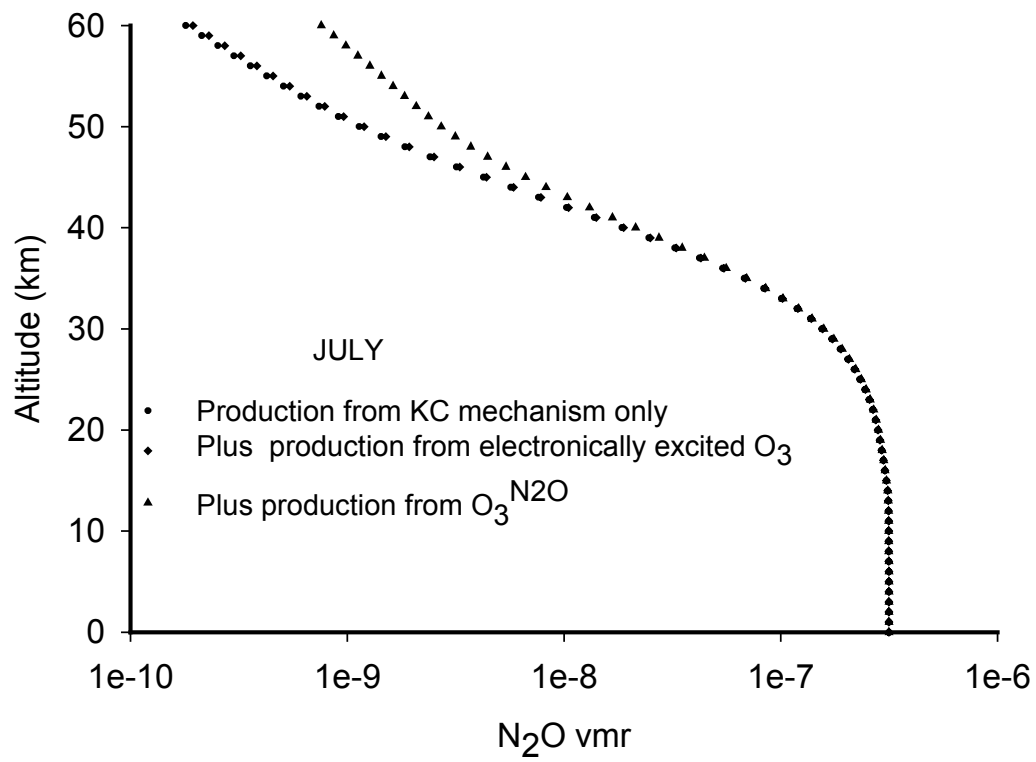


Figure 3

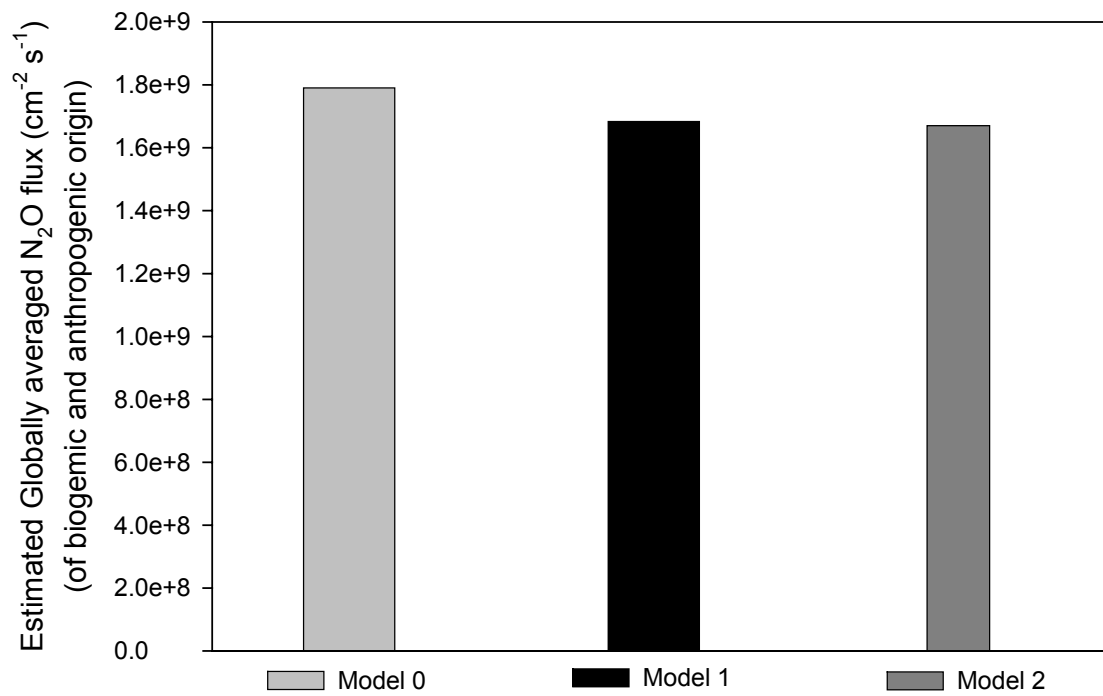


Figure 5

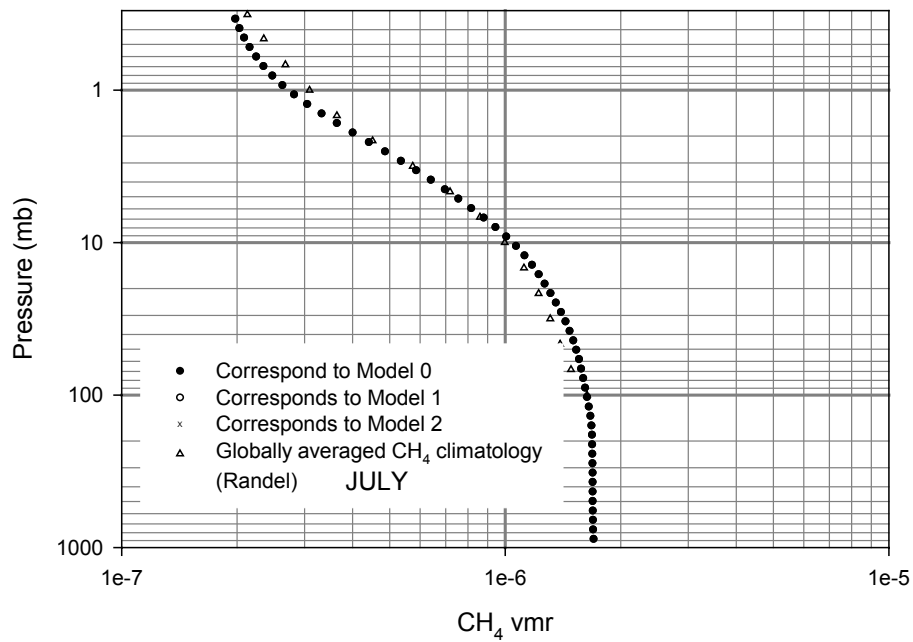
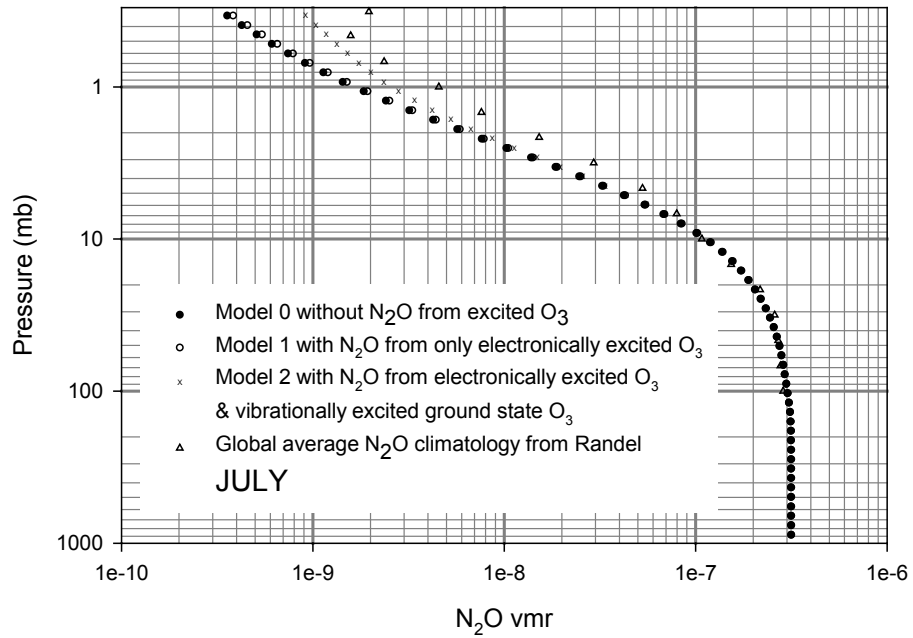


Figure 6

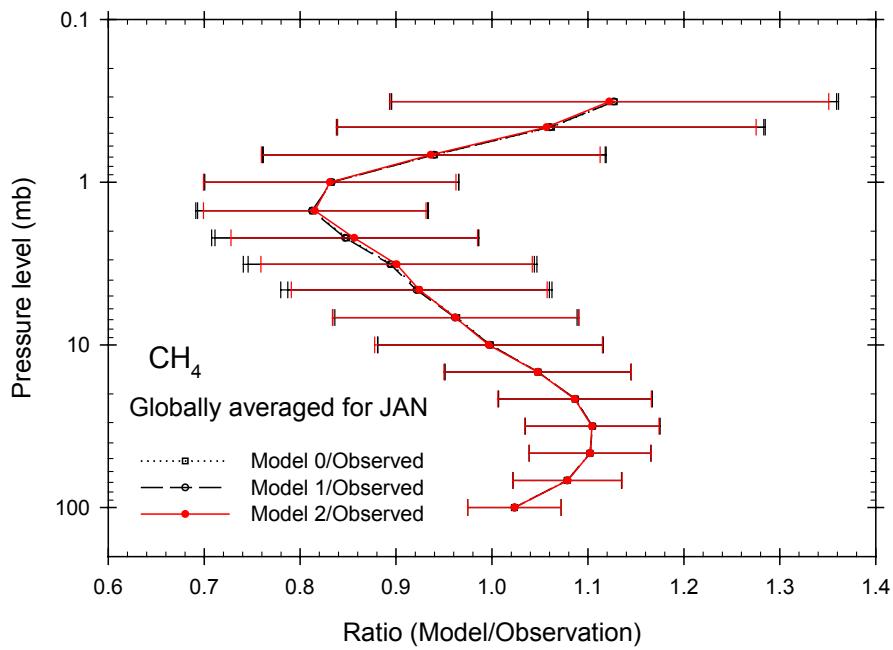
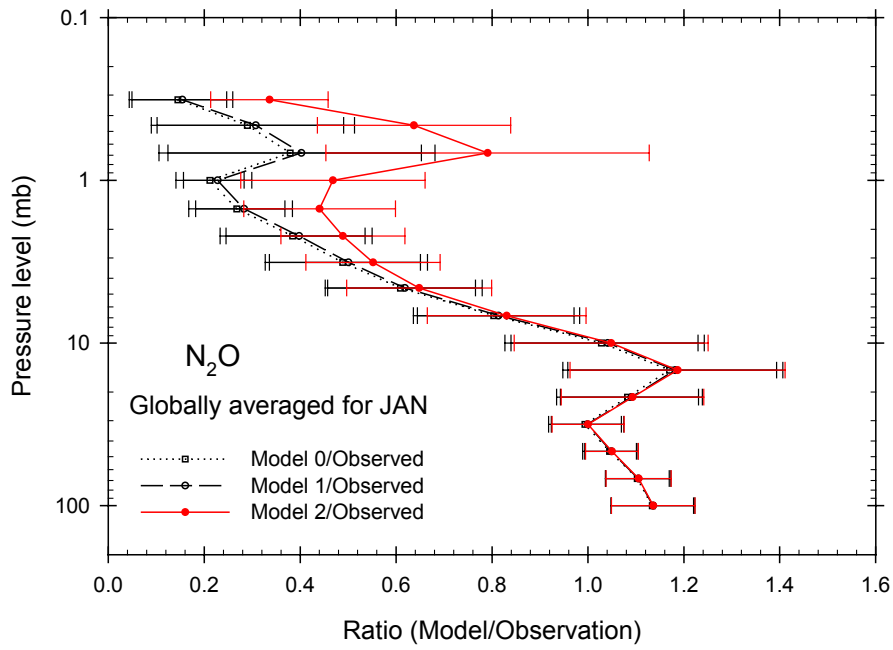


Figure 7

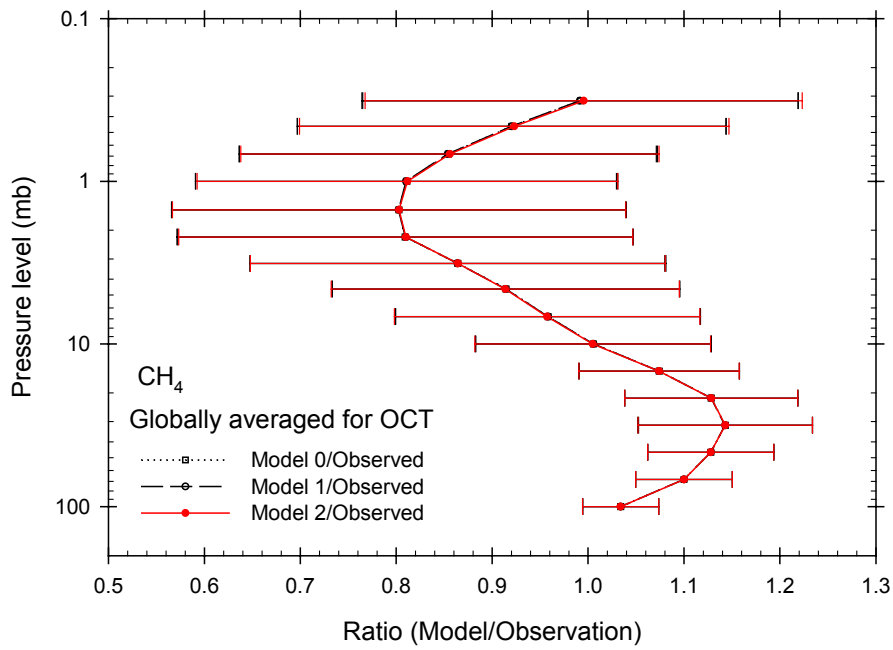
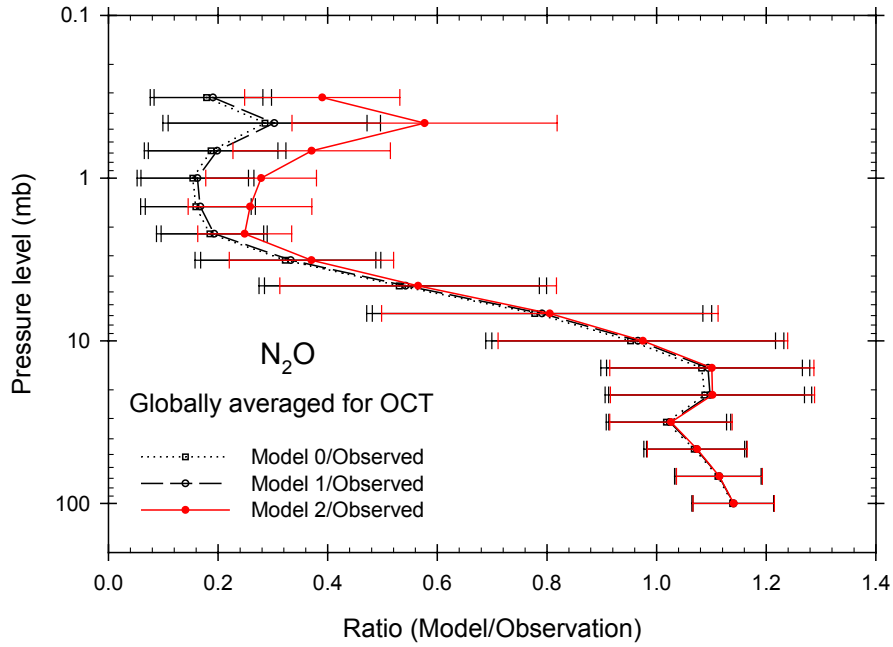


Figure 8